Nanostructured Nitrogen Doping TiO_2 Nanomaterials for Photoanodes of Dye-Sensitized Solar Cells

Wei Guo and Tingli Ma

Abstract This paper presents a review of nanostructured nitrogen doping (N-doped) TiO_2 nanomaterials and their application into dye-sensitized solar cells (DSCs). Such N-doped TiO_2 nanomaterials aim at enhancing the performance of TiO_2 photoanodes for DSCs. Herein, we summarize the different synthesis methods, nanostructures, and physiochemical properties of N-doped TiO_2. Also, the differences in electron transport behavior in DSCs based on N-doped and pure TiO_2 photoanodes were involved. Further understanding of the nanostructured N-doped TiO_2 photoanodes will promote the development of energy conversion and other related areas.

Keywords Dye-sensitized solar cell · Nitrogen-doped titania · Photoanode · Charge transport

1 Introduction

Dye-sensitized solar cells (DSCs) have been extensively studied for decades as a low-cost alternative to conventional silicon solar cells since they were reported by Grätzel and co-workers [1, 2]. Encouragingly, many improvements have been achieved by introducing new dyes, electrolytes, and different morphologies to the semiconductor materials [3]. The highest energy conversion efficiency of DSCs has reached to 12.3 % [3]. However, further improving the energy conversion efficiency of DSCs is important for successful commercialization. Photoanodes made of metal oxide semiconductor are known to be one of the key components that significantly affect the overall energy conversion efficiency of DSCs.

W. Guo · T. Ma (✉)
State Key Laboratory of Fine Chemicals, School of Chemical Engineering, Dalian University of Technology, Dalian 116024, People's Republic of China
e-mail: tinglima@dlut.edu.cn

Z. Lin and J. Wang (eds.), *Low-cost Nanomaterials*, Green Energy and Technology,
DOI: 10.1007/978-1-4471-6473-9_3,

Generally, nanocrystalline mesoporous metal oxide semiconductor (typically TiO_2) films, which adsorb dye molecules and transport photogenerated electrons to the outer circuit, serve as electron conductors and dictate the efficiency of electron transport and collection [4]. Therefore, the oxide semiconductor of photoanodes plays a key role in the performance of DSCs. Specifically, an excellent photoanode should include: (1) a large surface area and an appropriate isoelectric point (IEP) which can guarantee a high amount and quality of dye uptake; (2) a perfect lattice and low electron trap distribution to reduce the photogenerated electron losses; and (3) a good neck-connection between nanoparticles, which facilitate the electron transport during collection to the conductive substrate.

In recent years, nanocrystalline metal semiconductor materials are extensively studied for the mesoporous photoanodes of DSCs. Nanocrystalline mesoporous photoanodes made of TiO_2 materials, as one of the most widely used semiconductors, show an excellent performance in the DSCs. Some researchers also study other types of semiconductors, such as ZnO [5], Zn_2SnO_4 [6], WO_3 [7], $SrTiO_3$ [8], Nb_2O_5 [9], SnO_2 [10], CeO_2 [11], FeS [12], and NiO [13]. However, the photovoltaic performance of DSCs based on these semiconductor materials remains low because some of these materials are not stable in dye solution, such as ZnO and so on. On the other hand, some materials have a low isoelectric point (IEP), such as SnO_2, which is not suitable for dye molecular linking. However, these non-TiO_2 materials need to be further studied and developed to get a good photovoltaic performance for DSCs. Up till now, TiO_2 is still the best choice for photoanodes in DSCs. Aiming at the further improvement for DSCs, on the one hand, we can develop more efficient and diverse structures of TiO_2 materials. On the other hand, we can modify TiO_2 to enhance its performance, such as chemical doping. As oxygen deficiencies exist in pure TiO_2 crystal structures [14–16] these oxygen deficiencies can induce TiO_2 to a visible light absorption response producing electron-hole pairs. The photoexcited TiO_2 will lead to the oxidation of iodide or dye by photogenerated holes. Such deficiencies are possible causes for the shortened lifetime of DSCs. Element doping is an effective way to improve the performance of TiO_2. We can choose metal or nonmetal to proceed with TiO_2 doping. Recently, some studies reported the modifying of pure TiO_2 with metal doping, i.e., Zn-, La-, Ta-, and Nb-doped TiO_2 [17–20]. The performance of DSCs can be improved by adjusting doping metals. However, metal doping can affect the position of conduction band (CB) of TiO_2 contributing to the change in photovoltage. Besides, metal doping also introduces more recombination sites for electron [21]. Nonmetal doping of TiO_2 materials is another good choice for fine-tuning of TiO_2. Nonmetal elements, such as N [22, 23], C [24], B [25], I [26] etc., are used to dope TiO_2. Especially for DSCs, nitrogen seems to be the most effective element to enhance the photovoltaic performance of DSCs.

This review summarizes the recent works on the N-doped TiO_2 materials and their application into photoanodes of DSCs. Herein, the synthesis methods and optical properties of N-doped TiO_2 are introduced briefly. Then the effect of N-doped TiO_2 photoanodes on the performance of DSCs is described in detail. Finally, we discuss the charge transport in DSCs based on N-doped TiO_2 photoanodes.

2 Synthesis and Characterizations of Nanocrystalline N-Doped TiO_2

Various methods have been reported for the synthesis of N-doped TiO_2 since the study by Asahi et al. in 2001 [22]. The methods are generally classified as: (1) sintering TiO_2 at high temperatures under an N-containing atmosphere (NH_3 gas or mixeds), which we called dry methods [23, 27, 28]; (2) chemical wet methods, which involve sol–gel and solvothermal methods [29–32], some chemical nitrogen sources are added into water or alcohol during the hydrolysis of titanium alkoxide; and (3) sputtering and implantation deposition techniques, [33, 34] that were mainly used to prepare single crystalline or polycrystalline N-doped TiO_2 thin films. Herein, we emphasize the development of the former two methods that were used to fabricate N-doped TiO_2 photoanodes of DSCs.

2.1 Dry Methods

Dry method involves a high temperature sintering and doping process. This method can be easily controlled by adjusting the N-containing atmospheres and starting materials.

In 2005, our group reported the synthesis of N-doped TiO_2 employing the dry method. The starting pristine TiO_2 was commercial anatase powders (ST-01, Ishihara Sangyo Kaisha, Ltd.), which were treated at 550 °C for 3 h under a dry N_2 and NH_3 flow [23]. Interestingly, we obtained needle-like N-doped TiO_2 crystals with excellent thermostability. Afterwards, we also used P25 (Degussa) as the starting materials to obtain N-doped P25. These N-doped ST-01 and P25 materials show good performance over pristine TiO_2 photoanodes. Additionally, we also found that the starting materials apparently affect the N-doping effect from N-doping amount and optical properties. As reported earlier, the phase transition of anatase into rutile can occur at a high sintering temperature [35]. However, our nitridation process did not affect the crystal structure of pristine TiO_2, as shown in Fig. 1. Moreover, the obtained N-doped ST-01 showed excellent thermal stability. We can see in Fig. 2 the UV-Vis absorption spectra of N-doped ST-01 powders, treated under different conditions, which suggest that after being sintered separately in air, N_2, Ar, or at high temperature up to 700 °C, the N-doped ST-01 still shows visible light absorption, which is a signal for successful N-doping.

In 2009, Yang et al. developed a set of reaction devices for the process of thermal doping treatment [36]. The TiO_2 samples were treated with NH_3 under middle pressures and controlled conditions. This synthesis route is an effective approach to adjust the nitrogen concentration and band gap of N-doped TiO_2. They obtained a series of N-doped TiO_2 materials with different nitrogen doping amount by adjusting the temperature, pressure, and time. Moreover, the anatase type N-doped TiO_2 can be obtained at the sintering temperature of 400–500 °C. When the temperature increased to 600 °C, the rutile phase can be observed.

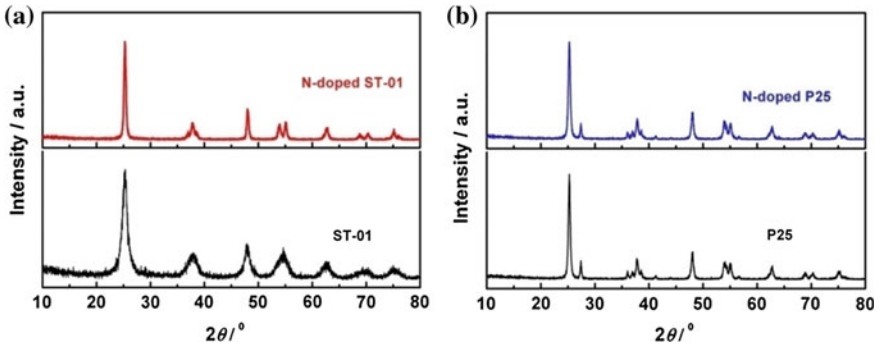

Fig. 1 X-ray diffraction patterns. **a** N-doped ST-01 and pristine ST-01 powders; **b** N-doped P25 and pristine P25 powders

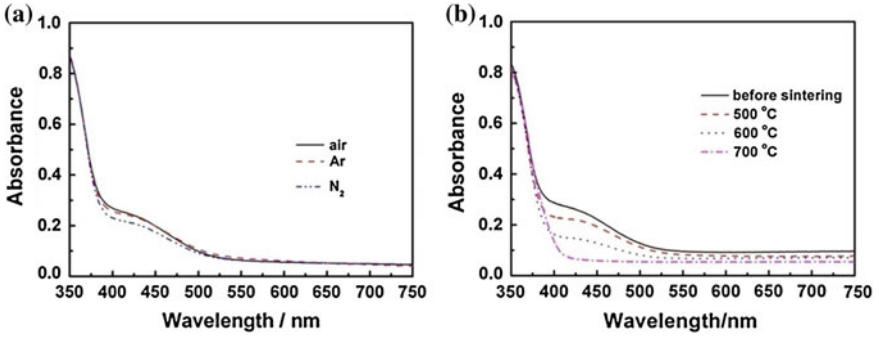

Fig. 2 UV-Vis absorption spectra of of N-doped ST-01 powders treated under different conditions: **a** in different sintering atmosphere; **b** at different temperature for 30 min [23]

The dry method is an aftertreatment process for N-doping which requires a high sintering temperature. Besides, this method can be controlled by adjusting the N-containing atmosphere and sintering temperature to get different N-doped TiO_2 materials. However, the high temperature sintering of TiO_2 may also lead to a degree of nanoparticles aggregation.

2.2 Chemical Wet Method

The wet method is widely used to synthesize TiO_2 nanomaterials. Until now, the wet method has been one the most successful methods for doping because of its convenient control of titanium sources, the nitrogen doping amount, and hydrolysis condition. In addition, simple variations in experimental conditions can lead to the required particle size and crystal structures, such as the hydrolysis rate of titanium alkoxide, pH of solvent solution, and solvent systems [37]. Besides, the

nitrogen sources can be also chosen to adjust the nitrogen doping process. Inorganic and organic nitrogen dopants (such as aqueous ammonia, urea, ammonium chloride, triethylamine, and diethylamine) are widely used in the synthesis of N-doped TiO_2.

Our group focused on the sol–gel wet method to investigate the types of nitrogen dopants and amount on the performance of the N-doped TiO_2, and thereby their photovoltaic performance of the DSCs. The sol–gel method usually involves two steps: (1) hydrolysis of titanium alkoxide in solvent (water or ethanol) containing nitrogen sources; and (2) sintering the obtained precipitate under 400–500 °C for a certain amount of time. However, we found that the nitridation process and doping amount varies with each N-doping method and type of nitrogen sources. We used ammonia, triethylamine, and urea nitrogen dopants to synthesize N-doped TiO_2 nanocrystals, which were denoted as N–A, N–U, and N–T, respectively [38–41]. By varying initial molar ratios of N/Ti, a series of N-doped TiO_2 with different N dopant amounts can be also synthesized according to the N-A method [42]. As the previous literature reported, we also found that the nitrogen doping process differs for the N-A, N-U, and N-T powders. During the preparation of N-A, nitrogen doping proceeded simultaneously with the hydrolysis of the titanium alkoxide. The hydrolysis of the titanium isopropoxide (TTIP) consisted of two steps [43]: hydrolysis and concentration. Titanium hydroxide was formed in the hydrolysis and was called titanic acid, which exhibits acidity. The titanic acid then reacted with NH_4OH to form ammonium titanate, which when heated, dehydrated and desorbed to NH_3 and allowed N-doping to occur. Ammonia in the doped samples becomes oxidized by the lattice oxygen, and this oxidation allows for the uptake of nitrogen. During the preparation of N-U, simultaneous N-doping with phase formation occurred by heating a mixture of titanium hydroxide and urea. When the mixture was heated, the urea was decomposed into NH_3 and CO_2, and the generated NH_3 reacted with the oxygen of the TiO_2 to form the N-doped TiO_2. The N-T sample was formed by direct nitridation of the anatase TiO_2 nanostructures with alkylammonium salt. In this case, triethylamine was used as the alkylammonium salt, and the N-T nanocrystals were obtained by controlling hydrolysis rate of the TTIP and the pH value of the solution. As a side note, some amine groups can coordinate to the central Ti ion early during the N-doping process, and these amine linkages can be hydrolyzed by the addition of a dilute solution of acid or base, but this addition in turn adjusts the pH of the reaction mixture. Therefore, high pH values are required. By using high pH values, the Ti-bound amine groups can be easily substituted by OH^- during the hydrolysis process, which results in the formation of N-doped TiO_2 nanoparticles. [40] Furthermore, the obtained different phases and crystallite sizes of N-doped TiO_2 can be ascribed to the different types of nitrogen dopants and to the hydrolysis of titanium alkoxide under controlled conditions. In the sol–gel wet method, the type of nitrogen sources not only influences the nitridation process but also the particle size and nitrogen concentration. The N dopant amounts were calculated using the XPS results and were found to be 2.77, 0.29, and 0.47 % for N-A, N-U, and N-T, respectively.

The solvothermal method is also an effective wet method to synthesis N-doped TiO_2. Dai et al. used urea as nitrogen source in the hydrolysis of TTIP [44]. The precipitation solution was treated in an autoclave at 200 °C for 10 h. They observed that the (101) peak positions of N-doped TiO_2 showed a shift compared with the undoped ones. This is also reported in Jagadale's work on N-doped TiO_2 by the sol–gel method [45].

Wet methods are the first choice to be employed to determine the suitable nitrogen dopants, and it is also a simple N-doping method. Therefore, it is necessary to seek an appropriate wet method, nitrogen sources, and N dopant amount for the large-scale production of N-doped TiO_2 nanomaterials.

2.3 Other Techniques

There are some other approaches for preparation of N-doping TiO_2 materials such as combustion, ion-implantation, and sputtering techniques.

Recently, Ogale and Gopinath et al. reported a disordered mesoporous framework of N-doped TiO_2 consisting of nanoparticles. They used a simple combustion synthesis method to prepare N-doped TiO_2 using $Ti(NO_3)_4$ as Ti precursor and urea as fuel. They found that urea/$Ti(NO_3)_4$ molar ratio of $\leqq 7$ leads to a biphasic (anatase and rutile) titania. A high ratio of urea/$Ti(NO_3)_4$ ($\geqq 9$) leads to exclusive anatase phase TiO_2. The pseudo-3D nature of mesoporous N-doped TiO_2 consisting of mesoporosity and electrically interconnected nanosized crystalline particles lead to a higher efficiency in DSCs [46].

Kang et al. reported an ion-implantation technique combination with electrostatic spray to prepare hierarchical nanostructured TiO_2 clumps doped by nitrogen-ion [47]. The ion-implantation could be a straightforward tool to implant foreign atoms into the lattice. This ion doping intrinsically modifies the lattice structure and consequently the properties of host counterparts [48].

Magnetron sputtering deposition method is also a widely used technique to prepare N-doped TiO_2 thin films. We can obtain the films by depositing Ti in plasma of argon, oxygen, and nitrogen. By varying the nitrogen contents in the flow, we can get a different nitrogen concentration within TiO_2 lattice from 2.0 to 16.5 % [49]. Early in 2003, Lindquist et al. used DC magnetron sputtering to prepare nanocrystalline porous N-doped TiO_2 thin films [50]. These films displayed a porous and rough surface. The crystal structure of N-doped TiO_2 thin films varying from rutile to anatase varied with the nitrogen content. However, the thickness of films only reached to several hundred nanometers.

Therefore, many methods can be used to synthesize nanocrystalline N-doped TiO_2. However, the crystal structure, surface property, and optical property of N-doped TiO_2 are all related to the synthesis methods.

2.4 Physical and Chemical Characterization of N-doped TiO_2

To evaluate the optical properties of N-doped TiO_2, UV-Vis spectrometry is the most commonly used technique to examine the doping effects on the host metal oxide matrix [51]. Generally, after N-doping treatment, the N-doped TiO_2 nanomaterials show a good visible light response between 400 and 500 nm. This trend is observed by many works. In our previous work, compared with pure TiO_2 and P25 electrodes, the N-doped TiO_2 samples (N-doped ST-01, N-doped P25) exhibited new absorption peaks in the visible light region between 400 and 550 nm (Fig. 3). However, intensity of the absorption response peaks show much dependence on the preparing conditions, such as N-doping amount as well as other related factors.

The reasons for the visible light response origin of N-doped TiO_2 are still open questions. Some work reported that the enhanced visible light absorption derived from band gap narrowing [52] (Fig. 4): (1) the localized dopant levels near the VB and the CB; (2) broadening of the VB; (3) localized dopant levels and electronic transitions to the CB. Then it was found that the Ti^{3+} defect or oxygen vacancies can also induce the redshift absorption. Giamello et al. [30] reported that N-doped TiO_2 electrodes contained N_b centers that were responsible for visible light absorption. Nevertheless, Serpone et al. [53] analyzed the DRS spectra (diffuse reflectance spectra) of anion- and cation-doped TiO_2 electrodes. They concluded that the absorption features in the visible light region originated from color centers developed during the doping process or post-treatments rather than by narrowing the intrinsic band gap for the TiO_2 electrode as originally proposed by Asahi and co-workers [22]. Burda et al. recently studied the electronic origins of the visible light absorption properties of C-, N-, and S-doped TiO_2 nanomaterials. They revealed that additional electronic states above the valence band edge existed, which could explain the redshift absorption of these materials [54]. On the basis of the above discussion, a conclusion doping mechanism is still needed to further understand the origin of visible light response.

X-ray photoelectron spectroscopy (XPS) is a powerful tool to get information about the electronic structure and chemical environment of the elements on the surface. So far, the XPS analysis is a surface characterization technique that could be affected by testing environment. The XPS result can be considered as a reference. Especially for N-doped TiO_2, XPS is the most reported technique to analyze the nitrogen concentration and chemical environment. What we concern most is three areas: the N 1s region, the Ti 2p region, and the O 1s region (Fig. 5).

For the N 1s region, the binding energy peaks ranged from 396 to 408 eV. However, the N 1s binding energy is highly dependent on the method of preparation. The peaks at 396 eV were not always observed. According to an earlier XPS study on the oxidation of pure TiN, the N 1s peak at 396 eV was assigned as the β-N in TiN; the 397.5 eV peak was due to the α-N_2, and the 400 eV and 405 eV peaks were assigned to the γ-N_2. In our previous work, we suggested to

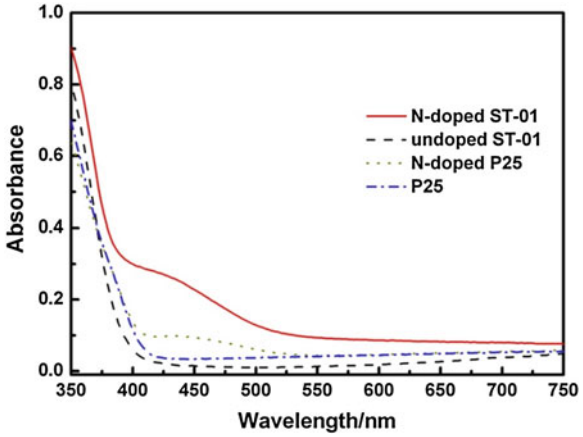

Fig. 3 UV-Vis absorption spectra of N-doped and undoped TiO_2 powders

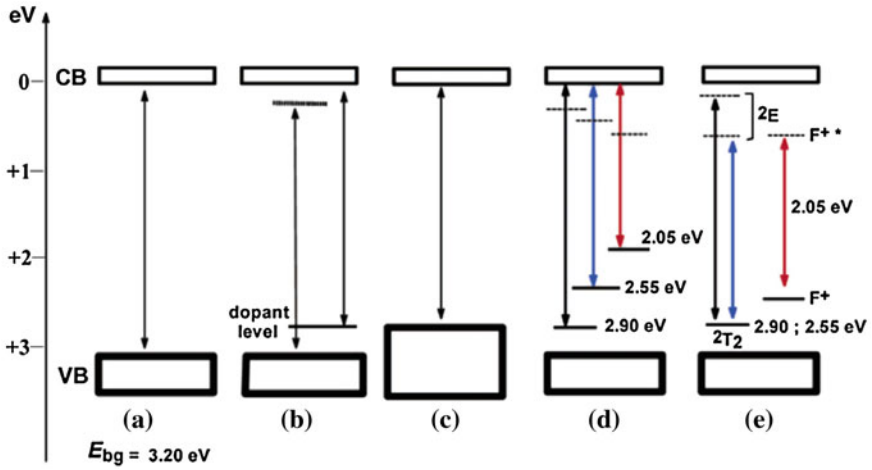

Fig. 4 Various schemes illustrating the possible changes that might occur to the band gap electronic structure of anatase TiO_2 on doping with various non-metals: **a** band gap of pristine TiO_2; **b** doped-TiO_2 with localized dopant levels near the VB and the CB; **c** band gap narrowing resulting from broadening of the VB; **d** localized dopant levels and electronic transitions to the CB; and **e** electronic transitions from localized levels near the VB to their corresponding excited states for Ti^{3+} and F^+ centers [52]

assign the peak around 398 eV to the O–Ti–N linkages in TiO_2 lattice [23]. Therefore, we concluded that nitrogen was doped into the TiO_2 lattices by substitution at the sites of the oxygen atoms. For the Ti 2p region, the Ti 2p3/2 and Ti 2p1/2 core levels appeared at 459 and 464 eV. For the O 1s region, the binding energies were around 530 eV. The Ti 2p and O 1s binding energies were similar to that in the pure TiO_2.

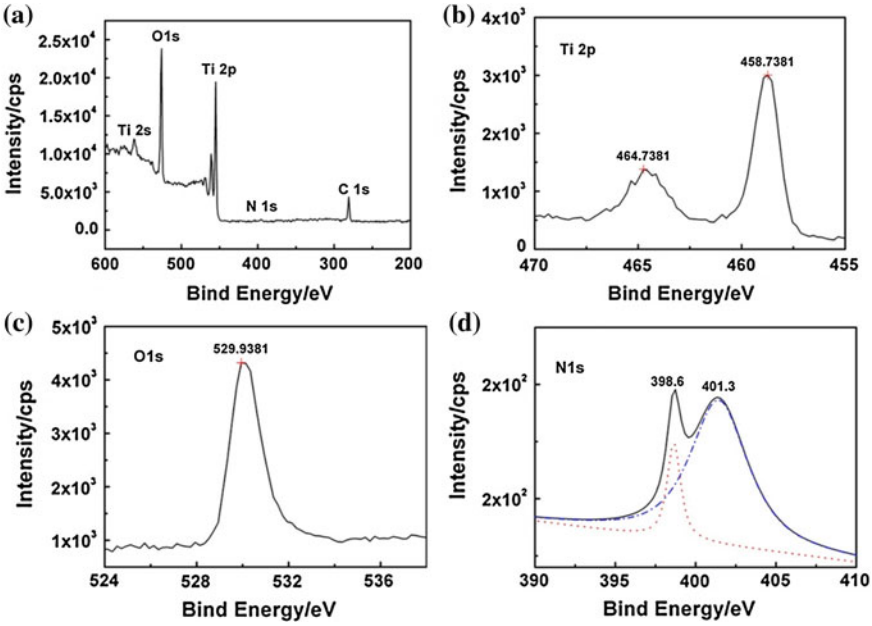

Fig. 5 XPS spectra of N-A-15: **a** survey; **b** Ti 2p; **c** O1s; d N1s [42]

3 Applications of N-doped TiO_2 into the DSCs

The porous semiconductor photoanode is an important part that influences the performance of DSCs. From the view of DSCs' photoanodes, the efficiency losses origin from photogenerated electron losses such as electron recombination during their transport to the substrate. The traps mainly come from the surface and lattice defect of TiO_2. Therefore, TiO_2 after nitrogen modifying is expected to decrease the electron losses. Our group and other researchers introduce N-doped TiO_2 to improve the performance of DSCs.

3.1 Effect of N-doping on the Overall Energy Conversion Efficiency

In our previous works, we reported highly efficient DSCs based on N-doped TiO_2 electrode (N-doped DSCs). The N-doped DSCs achieved a significant improvement in the energy conversion efficiency compared with the DSCs using P25 electrodes. Results show that N-doped TiO_2 electrodes could enhance the incident photo-to-current conversion efficiency (IPCE) and the overall conversion efficiency of the DSCs. Afterwards; we optimized the N-doped DSCs system, yielding a high efficiency of 10.1 % [55]. With careful evaluation of DSCs based on

N-doped and undoped TiO_2 prepared under the same dry method conditions, a 12.3 % enhancement of energy conversion efficiency was reached by N-doping. Then, we found that the nitrogen dopant type and amount influence the performance of N-doped TiO_2 photoanodes (Fig. 6) [56]. The different N dopants and wet methods affected the N-doping amount, the surface area of the N-doped TiO_2, and thereby the photovoltaic performance of the DSCs. By using the same nitrogen source (ammonia) and N-A wet method, it was found that the energy conversion efficiency of N-doped DSCs showed much dependence on the N dopant amount. A series of N-doped DSCs with different N dopant amounts showed the energy conversion efficiency of 5.01–7.27 %. Meanwhile, the pristine TiO_2-based DSCs showed an efficiency of 4.32 % only. Our work also showed that the fiber-type multiwall carbon nanotubes incorporated into N-doped TiO_2 electrode can enhance the electron collection efficiency of DSCs [57].

Yang et al. also reported the effect of N-doped amount on the performance of DSCs. Interestingly; they obtained three folds higher conversion efficiency for the optimum N-doped DSCs than the undoped ones, both J_{SC} and V_{OC} were improved [36]. In 2010, Sung et al. also reported the improvement of N-doped DSCs, which is due to the enhanced J_{SC} [58]. However, this N-doping effect is related to the synthesis method of N-doped TiO_2. In 2010, Dai et al. reported that through solvothermal treatment of N-doping process, the DSCs showed similar photovoltaic performance. However, the N-doped TiO_2 led to a more stable long-term stability and retarded electron recombination [44].

Overall, the N-doping modifying TiO_2 photoanodes contribute to the enhancement performance of DSCs either in J_{SC} or V_{OC}. We give a detailed discussion below.

3.2 *Effect of N-Doping TiO_2 on the Short-Circuit Current (J_{SC})*

A significant enhancement of J_{SC} was achieved for N-doped DSCs [23, 55, 56, 58]. Our work suggested that the significantly enhanced photocurrent of the devices was found to be related to the N dopant amount and the change in surface property, which affects dye uptake amount in N-doped TiO_2 electrodes. We investigated the amount of dye adsorbed on the electrodes. The J_{SC} of the N-A and N-U solar cells were higher than that of pure TiO_2 solar cells, although the N-A electrodes possessed almost the same amount of dye as pure TiO_2 electrodes did, while the N-U electrodes obtained a lower dye uptake than that of pure TiO_2 electrodes. On the other hand, the isoelectric points of TiO_2 have an effect on the dye-loading. Surfaces with higher isoelectric points are preferable for the attachment of dye with acidic carboxyl groups [59]. During the wet method synthesis of N-doped TiO_2 precursor, hydrolysis of TTIP was conducted in solvent containing nitrogen sources with weak alkaline. Therefore, we can speculate that the pH-dependent zeta potential and the isoelectric points of N-doped TiO_2 were changed.

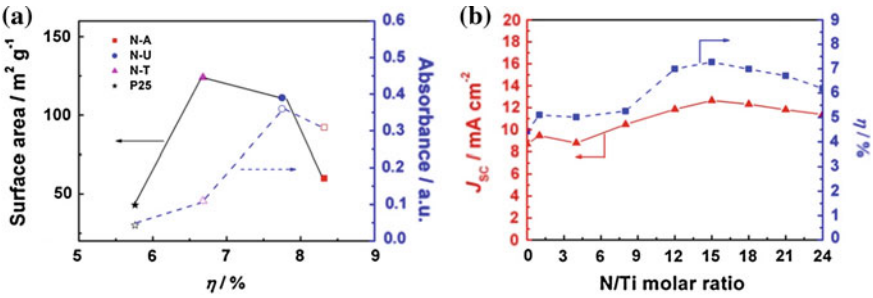

Fig. 6 **a** Effect of surface area and absorbance intensity (520 nm) on η [56]; **b** Effect of N/Ti molar ratio on J_{SC} and η [42]

Sung et al. also reported an enhanced photocurrent and efficiency in N-doped DSCs [58]; they attributed the enhancement to the increase of N-doped TiO_2 in the near-vis absorbance by nitrogen doping and partially to the morphological properties of the N-doped TiO_2 film. However, the visible light response of N-doped TiO_2 can only contribute photocurrent in tens of microamperes, which are far from enough to fill the gap caused by dye-sensitized films [55]. The efficient electron transport and retarded electron recombination can also lead to an increase in J_{SC} which will be discussed in the following section.

3.3 Effect of N-Doping TiO_2 on the Open-Circuit Voltage (V_{OC})

The increased V_{OC} of N-doped DSCs also enhanced the overall energy conversion efficiency. In theory, the V_{OC} of DSCs is determined by the difference between the Fermi level (E_F) of semiconductor and potential of redox couples [60]. It is helpful to get information about whether N-doping would cause a shift of E_F and thus the V_{OC}.

Dai et al. measured the V_{fb} of N-doped and undoped TiO_2 films [44]. They found that V_{fb} of N-doped TiO_2 shifts to the negative by 0.06 and 0.1 eV compared with that in the pure TiO_2 electrode (Fig. 7).

In the previous literature, Hashimoto et al. reported that the flatband potentials of N-doped TiO_2 tend to shift to a positive direction [61]. Kisch et al. observed that the quasi-Fermi level of electrons is anodically shifted by 0.07–0.16 eV [62]. Higashimoto et al. reported that the flatband potential of N-doped TiO_2 is not influenced by small amounts of nitrogen species doped into TiO_2 [63]. Therefore, there is still no conclusion about the change in E_F of TiO_2 after N-doping.

Our group used surface photovoltage spectroscopy (SPS) to measure the energy levels of bare N-doped TiO_2 films and dye-sensitized N-doped TiO_2 electrodes [55]. In Fig. 8a, we can see that an impurity level exists from where photoexcited electrons are injected into the conduction band, indicating that nitrogen is doped

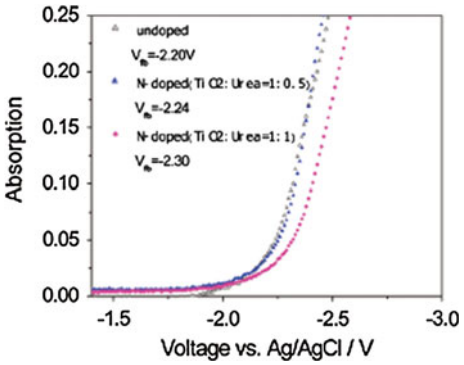

Fig. 7 Absorbance measured at 780 nm as a function of applied potential for Undoped and N-doped TiO_2 electrode [44]

into the TiO_2 lattice, where it forms nitrogen-induced states. In Fig. 8b, the observed signal starting at around 740 nm (scanning from long to short wavelength) for N-doped and undoped TiO_2 is due to electron injection from the N719 dye into the conduction band of TiO_2. We observed that the signal for dye-sensitized N-doped ST-01 with respect to the undoped ST-01 is blueshifted at about 20–40 nm. This result may indicate the shift in the electron quasi-Fermi level in N-doped TiO_2.

We further investigated the relationship between voltage and charge using a charge extraction technique [64]. The similar slope of voltage-charge plots of the N-doped and undoped TiO_2 solar cells (N-A and TiO_2 DSCs) indicate a similar trap distribution (Fig. 9). However, if sustaining a certain voltage, more charge needs to be present in the TiO_2-based DSCs. The relationship between charge and voltage revealed that less charge is needed to get a high V_{OC} in N-doped DSCs.

We also noticed that the increase in V_{OC} cannot always be observed, which is also dependent on the synthesis method of N-doped TiO_2. The synthesis method may influence the type of N-doping, such as lattice perfection, interstitial doping, or just physical adsorption. Therefore, much effort would be made to further understand the doping mechanism in energy level of N-doped TiO_2.

3.4 Long-Term Stability

In DSCs system, photoanodes made of TiO_2 nanomaterial are not photoexcited instead of dyes. However, N-doping would cause TiO_2 visible light absorption response, which is widely applied to photocatalysis area. Whether N-doped TiO_2 can possibly accelerate the deterioration of the dye or DSC system is always a concern.

The stability test for N-doped DSCs was conducted in our previous work (Fig. 10), N-doped DSCs were examined during irradiation for 2000 h under white light illumination (100 mW/cm^2) at 25 °C [23]. The N-doped DSCs possessed good stability with efficiency and photovoltage maintaining its initial values above 90 %. Dai group also reported great stability of N-doped DSCs, the efficiency of

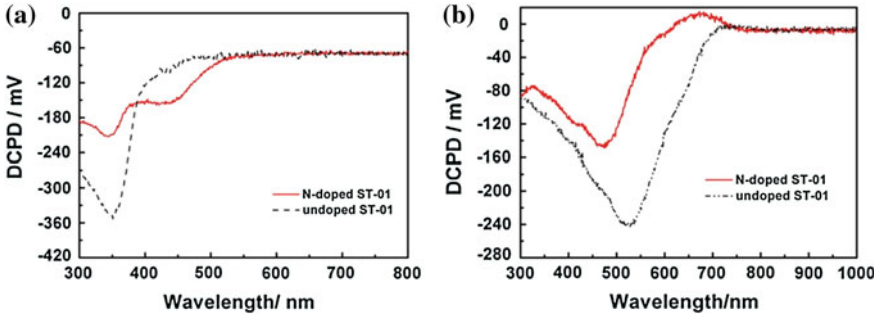

Fig. 8 Surface photovoltage spectra: **a** bare N-doped and undoped ST-01 electrodes and **b** after N719-sensitization [55]

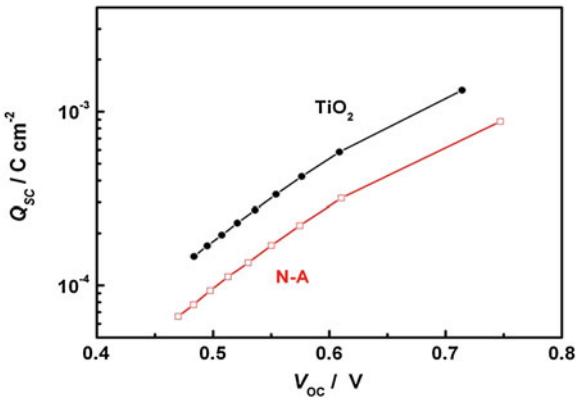

Fig. 9 V_{OC} versus Q_{SC} (N-A: N-doped DSCs) [56]

which remained at nearly at 80 % compared with the 72 % of the undoped DSC at 70 °C over 1,000 h [44].

Further investigation on the effect of N-doped TiO_2 on the deterioration of the dye was also performed [55]. The dye stability tests consisted of examining the dyes adsorbed on the N-doped TiO_2 films and the photoanodes of the solar cells. In Fig. 11a, compared with UV-Vis absorption spectra of fresh N719, the dyes desorbed from N-doped and undoped TiO_2 film were destroyed but to a similar extent. In Fig. 11b, the absorption of fresh dye is almost the same with those in N-doped and undoped TiO_2 photoanodes. These results indicate that N-doped TiO_2 did not accelerate the dye deteriorations.

3.5 Application of N-doped TiO_2 Photoanodes into QDSCs

Except for DSCs, N-doped TiO_2 nanomaterials were also applied into quantum-dot sensitized solar cells (QDSCs).

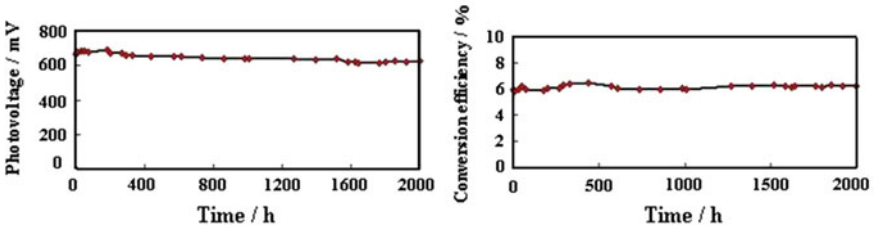

Fig. 10 Long-term stability of the DSCs based on $TiO_{2-x}N_x$ electrode [23]

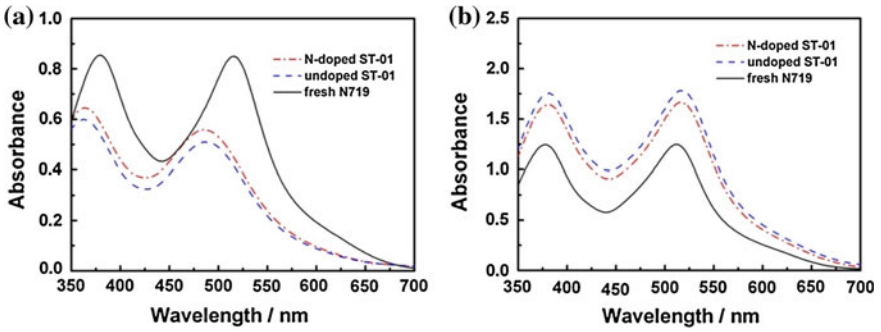

Fig. 11 UV-Vis absorption spectra of **a** fresh N19 dye and the dyes desorbed from N-doped and undoped ST-01 films; **b** fresh N19 dye and the N719 dye desorbed from N-doped and undoped DSCs devices [55]

Zhang et al. combined N-doped TiO_2 and CdSe QDs to assemble QDSCs. Compared with QDSCs using pristine TiO_2, the photocurrent of CdSe-sensitized N-doped TiO_2 QDSCs was significantly enhanced. They ascribed this photocurrent enhancement to the extra pathways for charge transfer introduced by nitrogen doping (Fig. 12) [65]. Kang et al. reported the hierarchical N-doped TiO_2 nanoclumps as photoanodes of CdSe-sensitized QDSCs. They found that the performance of QDSCs was improved by 145 % when using N-ion doping of TiO_2 photoanodes. One of the two explanations about the significant improvement of QDSCs was the increased recombination resistance at TiO_2/QDs/electrolyte interface, which was caused by the decreased surface states and oxygen vacancies after nitrogen doping in TiO_2 [47].

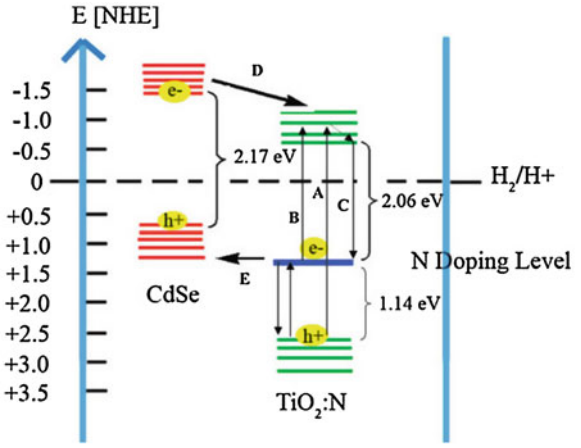

Fig. 12 Schematic electronic band structure of 3.5 nm CdSe with an effective band gap of 2.17 eV and nanocrystalline TiO_2/N with a 3.2 eV band gap [65]

4 Electron Kinetic Behaviors in DSCs Based on N-doped TiO_2 Photoanodes

4.1 Charge Transport and Electron Lifetime

Understanding electron transport in the N-doped DSCs is helpful to further improve the performance of semiconductor photoanodes. We investigated the charge transport by intensity-modulated photocurrent and photovoltage spectroscopy (IMPS/IMVS) to study the effect of N-doping treatment [55]. Usually, IMPS/IMVS measurements were affected by particle size in correlation with surface area and morphology, resulting in differences in the number of particles and the quantity of the charge associated with that electrode. When comparing the doped samples with pure samples, we needed to assure they possessed similar particle sizes and surface area to obtain comparability results. Therefore, we studied the N-doping effect by using the N-doped DSCs (N-A) solar cells and pure TiO_2 solar cells, which had similar particle sizes (22.74 and 23.13 nm, respectively).

The electron transport time (τ_{tr}) and electron lifetime (τ_e) were deduced from IMPS and IMVS results (Fig. 13) [55]. All of the time constants followed a general trend; they decreased as the light intensity increased. Fast electron transport and short electron lifetime existed for the N-A. Commonly, fast electron transport can improve the charge-collection efficiency and thus increase the J_{SC}. In general, N-doping would cause some defects in TiO_2 lattice, which would cause more traps in the doped films. However, we observed similar slopes, suggesting similar trap distributions.

V_{OC} decay measurements were performed to further clarify the electron lifetime. As shown in Fig. 14a, the V_{OC} decay is slightly different in the N-A DSCs, which follows the sequence of N-A > pure TiO_2. Additionally, the decay is faster in the N-A solar cell, which is also in agreement with the shorter lifetime found in

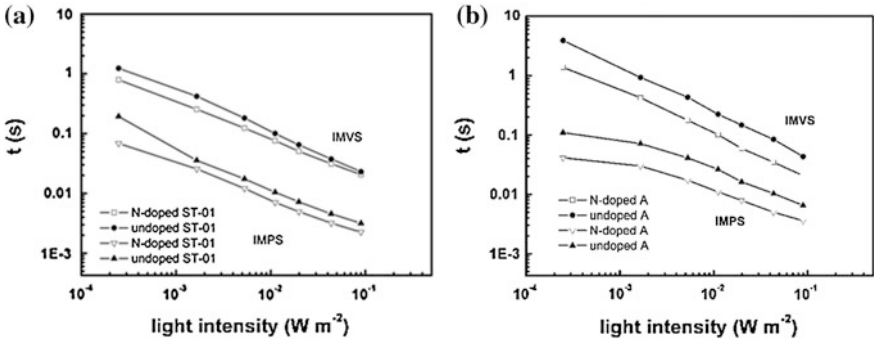

Fig. 13 IMPS time constants as functions of light intensity for N-doped and TiO_2 DSCs [55]

the N-A DSCs (Fig. 14b). The electron lifetime can be calculated from the voltage transients using Eq. (1) [56]:

$$\tau_e = -\frac{kT}{e}\left(\frac{dVoc}{dt}\right)^{-1} \tag{1}$$

where k is the Boltzmann constant, T the absolute temperature, and e the positive elementary charge. The calculated electron lifetimes are shown in Fig. 14b as functions of the open-circuit potential. Specifically, the lifetimes increased exponentially when the voltage decreased. However, the lifetime of the N-A solar cell was shorter than in the pure TiO_2 solar cells at $U < 0.6$ V, but it was longer when $U > 0.6$ V.

The electron lifetime can also be deduced from EIS spectra. The electron lifetime can be estimated by the maximum frequency in the EIS spectra as described: $\tau_e = (2\pi f_{max})^{-1}$ [47]. We conducted a linear fit of electron lifetime, which tended to decrease as the N/Ti molar ratio increased (Fig. 14c).

Therefore, the N-doping treatment can improve the electron transport but decrease the electron lifetime in DSCs.

4.2 Electron Recombination

The difference between N-doped DSCs and TiO_2 DSCs with respect to their charge transfer properties was also studied by EIS analysis [47–49]. The Nyquist diagram typically features three semicircles in order of increasing frequency. These three semicircles correspond to the following: the Nernst diffusion within the electrolyte, electron transport at the oxide/electrolyte interface, and redox reaction at the platinum counter electrode.

The main concerns in N-doped DSCs are the following: (1) the impedance due to electron transfer from the conduction band of the mesoscopic film to triiodide

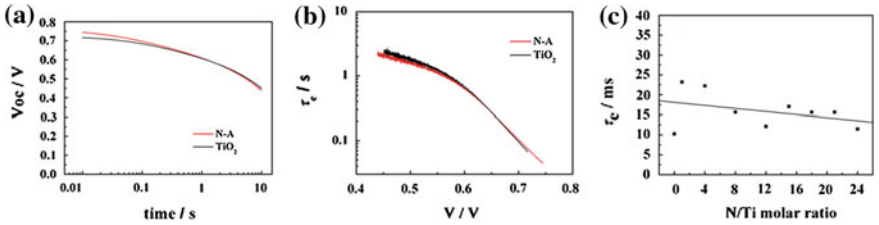

Fig. 14 **a** Open-circuit voltage decay transients of the dye-sensitized N-doped and pure TiO_2 solar cells; **b** calculated electron lifetime (Eq 1) versus open-circuit voltage [56]; **c** τ_e versus N/Ti molar ratio [42]

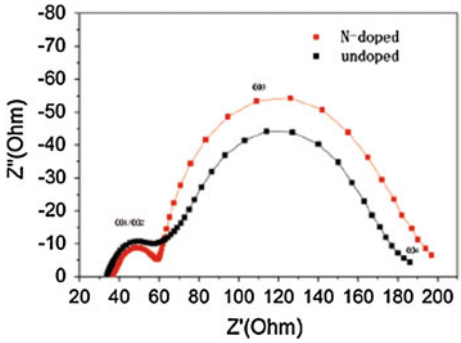

Fig. 15 EIS spectra of N-doped DSCs [44]

ions in the electrolyte and (2) the back reaction at the TiO_2/electrolyte interface, presented by the semicircle in intermediate-frequency regime. Dai et al. reported a retarded electron recombination in the N-doped DSCs. This retarded electron recombination may be due to the change in surface properties, e.g., the lattice perfection (Fig. 15). The charge transfer resistances demonstrated dependency on the N dopant amount. The electron lifetime of N-doped DSCs tended to decrease as the N dopant increased.

Overall, fast electron transport, short electron lifetime, and retarded electron recombination were found in N-doped DSCs. Moreover, a synergistic effect of high dye uptake and efficient electron transport contributed to the improvement of N-doped DSCs.

5 Summary and Outlook

In conclusion, the recent development of N-doped TiO_2 nanomaterials and its application into DSCs is summarized. The different synthesis approaches, nitrogen dopant types, and amount can affect the physical and chemical properties of N-doped TiO_2, thereby their performance in the photoanodes of DSCs. Moreover, nitrogen doping can help charge separation and transport in QDSCs. Based on these results, the synergistic effect of higher dye uptake, N dopant amount, and

faster electron transport contributed to the enhanced performance of N-doped DSCs. Therefore, N-doped TiO_2 nanomaterials are good semiconductor candidates for highly efficient photoanodes of DSCs. The application of N-doped TiO_2 is also widely extended into photocatalysis and other areas.

The fundamental research on how nitrogen doping enhances the charge transport and photovoltaic performance is still needed. Besides, the controlling of nanostructure and doping process of N-doped TiO_2 is an interesting topic in the future.

Acknowledgements This work was supported by NSFC (Grant No. 50773008) and State Key Laboratory of New Ceramic and Fine Processing (Tsinghua University). This work was also supported by the National High Technology Research and Development Program for Advanced Materials of China (Grant No. 2009AA03Z220).

References

1. O'Regan B, Grätzel M (1991) A low-cost, high-efficiency solar cell based on dye-sensitized colloidal TiO_2 films. Nature 353:737–740
2. Wang Q, Ito S, Grätzel M et al (2006) Characteristics of high efficiency dye-sensitized solar cells. J Phys Chem B 110:25210–25221
3. Yella H-W, Lee HN, Tsao C et al (2011) Porphyrin-sensitized solar cells with cobalt (II/III)-based redox electrolyte exceed 12 percent efficiency. Science 334:629–634
4. Grätzel M (2001) Photoelectrochemical cells. Nature 414(6861):338–344
5. Zhang Q, Chou TP, Russo B et al (2008) Aggregation of ZnO nanocrystallites for high conversion efficiency in dye-sensitized solar cells. Angew Chem Int Ed 47:2402–2406
6. Lana-Villarreal T, Boschloo G, Hagfeldt A (2007) Nanostructured zinc stannate as semiconductor working electrodes for dye-sensitized solar cells. J Phys Chem C 111:5549–5556
7. Zheng H, Tachibana Y, Kalantar-zadeh K (2010) Dye-sensitized solar cells based on WO_3. Langmuir 26:19148–19152
8. Yang S, Kou H, Wang J et al (2010) Tunability of the band energetics of nanostructured $SrTiO_3$ electrodes for dye-sensitized solar cells. J Phys Chem C 114:4245–4252
9. Sayama K, Sugihara H, Arakawa H (1998) Photoelectrochemical properties of a porous Nb_2O_5 electrode sensitized by a ruthenium dye. Chem Mater 10:3825–3832
10. Qian JF, Liu P, Xiao Y et al (2009) TiO_2-coated multilayered SnO_2 hollow microspheres for dye-sensitized solar cells. Adv Mater 21:3663–3667
11. Turković, Z. Crnjak Orel Z (1997) Dye-sensitized solar cell with CeO_2 and mixed CeO_2/SnO_2 photoanodes. Solar Energy Mater Solar Cells 45:275–281
12. Hu Y, Zheng Z, Jia H et al (2008) Selective Synthesis of FeS and FeS_2 nanosheet films on iron substrates as novel photocathodes for tandem dye-sensitized solar cells. J Phys Chem C 112:13037–13042
13. Qin P, Linder M, Brinck T et al (2009) High incident photon-to-current conversion efficiency of P-type dye-sensitized solar cells based on NiO and organic chromophores. Adv Mater 21:2993–2996
14. Inakamura N, Negishi S Kutsuna et al (2000) Role of oxygen vacancy in the plasma-treated TiO_2 photocatalyst with visible light activity for NO removal. J Mol Catal A: Chem 161:205–212

15. Ihara T, Miyoshi M, Iriyama Y et al (2003) Visible-light-active titanium oxide photocatalyst realized by an oxygen-deficient structure and by nitrogen doping. Appl Catal B-Environ 42:403–409
16. Irie H, Watanabe Y, Hashimoto K (2003) Nitrogen-concentration dependence on photocatalytic activity of $TiO_{2-x}N_x$ powders. J Phys Chem B 107:5483–5486
17. Wang K-P, Teng H (2009) Zinc-doping in TiO_2 films to enhance electron transport in dye-sensitized solar cells under low-intensity illumination. Phys Chem Chem Phys 11:9489–9496
18. Zhang Z, Zhao X, Wang T et al (2010) Increasing the oxygen vacancy density on the TiO_2 surface by La-doping for dye-sensitized solar cells. J Phys Chem C 114:18396–18400
19. Liu H, Yang W, Tan X et al (2010) Photovoltaic performance improvement of dye-sensitized solar cells based on tantalum-doped TiO_2 thin films. Electrochim Acta 56:396–400
20. Lu X, Mou X, Wu J (2010) Improved-performance dye-sensitized solar cells using Nb-doped TiO_2 electrodes: efficient electron injection and transfer. Adv Func Mater 20:509–515
21. Zhang X, Wang S-T, Wang Z-S (2011) Effect of metal-doping in TiO_2 on fill factor of dye-sensitized solar cells. Appl Phys Lett 99:113503
22. Asahi R, Morikawa T, Ohwaki T et al (2001) Visible-light photocatalysis in nitrogen-doped titanium oxides. Science 293:269–271
23. Ma T, Akiyama M, Abe E et al (2005) High-efficiency dye-sensitized solar cell based on a nitrogen-doped nanostructured titania electrode. Nano Lett 5:2543–2547
24. Hou Q, Zheng Y, Chen J-F et al (2011) Visible-light-response iodine-doped titanium dioxide nanocrystals for dye-sensitized solar cells. J Mater Chem 21:3877–3883
25. Tian H, Hu L, Zhang C et al (2011) Enhanced photovoltaic performance of dye-sensitized solar cells using a highly crystallized mesoporous TiO_2 electrode modified by boron doping. J Mater Chem 21:863–868
26. Chu D, Yuan X, Qin G et al (2008) Efficient carbon-doped nanostructured TiO_2 (anatase) film for photoelectrochemical solar cells. J Nanopart Res 10:357–363
27. Irie H, Washizuka S, Yoshinob N et al (2003) Visible-light induced hydrophilicity on nitrogen-substituted titanium dioxide films. Chem Commun 1298–1299
28. Fu H, Zhang L, Zhang S et al (2006) Electron spin resonance spin-trapping detection of radical intermediates in N-doped TiO_2-assisted photodegradation of 4-chlorophenol. J Phys Chem B 110:3061–3065
29. Burda C, Lou Y, Chen X et al (2003) Enhanced nitrogen doping in TiO_2 nanoparticles. Nano Lett 3:1049–1051
30. Livraghi S, Paganini MC, Giamello E et al (2006) Origin of photoactivity of nitrogen-doped titanium dioxide under visible light. J Am Chem Soc 128:15666–15671
31. Mrowetz Balcerski W, Colussi AJ et al (2004) Oxidative power of nitrogen-doped TiO_2 photocatalysts under visible illumination. J Phys Chem 108:17269–17273
32. Etacheri V, Seery MK, Hinder SJ et al (2010) Highly visible light active $TiO_{2-x}N_x$ heterojunction photocatalysts. Chem Mater 22:3843–3853
33. Torres GR, Lindgren T, Lu J et al (2004) Photoelectrochemical study of nitrogen-doped titanium dioxide for water oxidation. J Phys Chem B 108:5995–6003
34. Kitano K, Funatsu M et al (2006) Preparation of nitrogen-substituted TiO_2 thin film photocatalysts by the radio frequency magnetron sputtering deposition method and their photocatalyticreactivity under visible light irradiation. J Phys Chem B 110:25266–25272
35. Zhang J, Li M, Feng Z et al (2006) UV Raman spectroscopic study on TiO_2. I. Phase transformation at the surface and in the bulk. J Phys Chem B 110:927–935
36. Wang X, Yang Y, Jiang Z et al (2009) Preparation of TiNxO2−x photoelectrodes with NH_3 under controllable middle pressures for dye-sensitized solar cells. Eur J Inorg Chem 2009:3481–3487
37. Zhang J, Wu Y, Xing M (2010) Development of modified N doped TiO_2 photocatalyst with metals, nonmetals and metal oxides. Energy Environ Sci 3:715–726
38. Nakamura R, Tanaka T, Nakato Y (2004) Mechanism for visible light responses in anodic photocurrents at N-doped TiO_2 film electrodes. Phys Chem B 108:10617–10620

39. Kobayakawa K, Murakami Y, Sato Y (2005) Visible-light active N-doped TiO_2 prepared by heating of titanium hydroxide and urea. J Photochem Photobiol A: Chem 170:177–179
40. Chen X, Lou Y, Samia ACS et al (2005) Formation of oxynitride as the photocatalytic enhancing site in nitrogen-doped titania nanocatalysts: comparison to a commercial nanopowder. Adv Mater 15:41–49
41. Guo W, Miao Q, Xin G et al (2011) Dye-sensitized solar cells based on nitrogen-doped titania. Key Eng Mater 451:21–27
42. Guo W, Shen Y, Wu L et al (2011) Effect of N dopant amount on the performance of N-doped TiO_2 electrodes for dye-sensitized solar cells. J Phys Chem C 115:21494–21499
43. Sato S, Nakamura R, Abe S (2005) Visible-light sensitization of TiO_2 photocatalysts by wet-method N doping. Appl Catal A Gen 284:131–137
44. Tian H, Hu L, Zhang C et al (2010) Retarded charge recombination in dye-sensitized nitrogen-doped TiO_2 solar cells. J Phys Chem C 114:1627–1632
45. Jagadale TC, Takale SP, Sonawane RS et al (2008) N-doped TiO_2 nanoparticle based visible light photocatalyst by modified peroxide sol−gel method. J Phys Chem C 112:14595–14602
46. Sivaranjani K, Agarkar S, Ogale SB et al (2012) Toward a quantitative correlation between microstructure and DSSC efficiency: a case study of $TiO_{2-x}N_x$ nanoparticles in a disordered mesoporous framework. J Phys Chem C 116(3):2581–2587
47. Sudhagar P, Asokan K, Ito E et al (2012) N-ion-implanted TiO_2 photoanodes in quantum dot-sensitized solar cells. Nanoscale 4:2416–2422
48. Stroud PT (1972) Ion bombardment and implantation and their application to thin films. Thin Solid Films 11:1–26
49. Kitano M, Funatsu K, Matsuoka M et al (2006) Preparation of nitrogen-substituted TiO_2 thin film photocatalysts by the radio frequency magnetron sputtering deposition method and their photocatalytic reactivity under visible light irradiation. J Phys Chem B 110:25266–25272
50. Lindgren T, Mwabora JM, Avendaño E et al (2003) Photoelectrochemical and optical properties of nitrogen doped titanium dioxide films prepared by reactive DC magnetron sputtering. J Phys Chem B 107:5709–5716
51. Qiu X, Burda C (2007) N-doped TiO_2: theory and experiment. Chem Phys 339:44–56
52. Serpone N (2006) Is the band gap of pristine TiO_2 narrowed by anion- and cation-doping of titanium dioxide in second-generation photocatalysts? J Phys Chem B 110:24287–24297
53. Kuznetsov VN, Serpone N (2006) Visible light absorption by various titanium dioxide specimens. J Phys Chem B 110:25203–25209
54. Chen X, Burda C (2008) The electronic origin of the visible-light absorption properties of C-, N- and S-doped TiO_2 nanomaterials. J Am Chem Soc 130:5018–5019
55. Guo W, Wu L, Chen Z et al (2011) Highly efficient dye-sensitized solar cells based on nitrogen-doped titania with excellent stability. J Photochem Photobiol A Chem 219:180–187
56. Guo W, Shen Y, Boschloo G et al (2011) Influence of nitrogen dopants on N-doped TiO_2 electrodes and their applications in dye-sensitized solar cells. Electrochim Acta 56:4611–4617
57. Guo W, Shen Y, Wu L et al (2011) Performance of dye-sensitized solar cells based on MWCNT/TiO2–xNx nanocomposite electrodes. Eur J Inorg Chem 2011:1776–1783
58. Kang SH, Kim HS, Kim J-Y et al (2010) Enhanced photocurrent of nitrogen-doped TiO_2 film for dye-sensitized solar cells. Mater Chem Phys 124:422–426
59. Kay A, Grätzel M (2002) Dye-sensitized core—shell nanocrystals: improved efficiency of mesoporous tin oxide electrodes coated with a thin layer of an insulating oxide. Chem Mater 14:2930–2935
60. Cahen D, Hodes G, Grätzel M et al (2000) Nature of photovoltaic action in dye-sensitized solar cells. J Phys Chem B 104:2053–2059
61. Irie H, Washizuka S, Watanabe Y et al (2005) Photoinduced hydrophilic and electrochemical properties of nitrogen-doped TiO_2 films. J Electrochem Soc 152:351–356
62. Kisch H, Sakthivel S, Janczarek M et al (2007) A low-band gap, nitrogen modified titania visible-light photocatalyst. J Phys Chem C 111:11445–11449

63. Higashimoto S, Azuma M (2009) Photo-induced charging effect and electron transfer to the redox species on nitrogen-doped TiO_2 under visible light irradiation. Appl Catal B Environ 89:557–562
64. Duffy W, Peter LM, Rajapakse RMG et al (2000) A novel charge extraction method for the study of electron transport and interfacial transfer in dye sensitised nanocrystalline solar cells. Electrochem Commun 2:658–662
65. López-Luke T, Wolcott A, Xu L et al (2008) Nitrogen-doped and CdSe quantum-dot-sensitized nanocrystalline TiO_2 films for solar energy conversion applications. J Phys Chem C 112:1282–1292